

# Characterization, antimicrobial and catalytic activities of silver nanoparticles biosynthesized using aqueous extract of *Euphorbia graminea*

Olusegun E. THOMAS<sup>1\*</sup>, Olumuyiwa S. ALABI<sup>2</sup>, Patience E. OSHARODE<sup>1</sup>

<sup>1</sup> Department of Pharmaceutical Chemistry, Faculty of Pharmacy, University of Ibadan, Ibadan, Nigeria

<sup>2</sup> Department of Pharmaceutical Microbiology, Faculty of Pharmacy, University of Ibadan, Ibadan, Nigeria

---

## ABSTRACT

Phytosynthesis of silver nanoparticles (AgNPs) is not only affordable and eco-friendly but provides a means of synthesizing phytochemical capped AgNPs with predefined characteristics. The objective of this study was the green synthesis of AgNPs that possess antimicrobial and catalytic activities using aqueous extract of *Euphorbia graminea*. Reaction parameters critical to the yield, size and morphology of the biosynthesized AgNPs were optimized using UV spectroscopy. The UV-visible spectra analysis of the biosynthesized AgNPs showed surface plasmon resonance occurred at 462 nm. Scanning Electron Microscopy with Energy dispersive X-ray analysis revealed the characteristic absorption band of AgNPs at 3 KeV and confirmed 73.66% composition of particles as metallic silver. The AgNPs appeared as well-separated, quasi-spherical particles with narrow size distribution of  $6.77 \pm 0.89$  nm when examined with Transmission electron microscopy. X-ray diffraction confirmed the crystallinity of the AgNPs with mean crystallite size of 7.65 nm. The biosynthesized AgNPs showed broad-spectrum antimicrobial activity against bacteria and fungi. The rate constant of the degradation of methylene blue in the presence of as-synthesized AgNPs was increased several folds to  $\text{sec}^{-1}$  from  $\text{sec}^{-1}$  in its absence. The prepared AgNPs could find applications as therapeutic coats in medical devices and in effluent treatment of chemical industries.

**Keywords:** Silver nanoparticles, methylene blue, catalytic activity, antimicrobial activity, *Euphorbia graminea*

---

\*Corresponding Author: E-mail: seguntom@yahoo.com

ORCID:

Olusegun E THOMAS: 0000-0001-8519-2125

Olumuyiwa S ALABI: 0000-0003-0671-252X

Patience E OSHARODE: 0000-0002-5110-1683

(Received 25 Apr 2022, Accepted 07 Mar 2023)

## INTRODUCTION

Nanotechnology involves the manufacture, control of characteristics and applications of structures with nanoscale dimensions, typically between 1-100nm<sup>1</sup>. Nanoparticles are broadly of two types, which are the carbon-incorporated organic structures, and the more varied inorganic nanoparticles that include semi-conductor, metallic and magnetic nanoparticles. Metal nanoparticles because of their increased surface-to-volume ratio exhibit significantly altered physical, chemical and biological characteristics. Silver nanoparticles (AgNPs) for example, have substantial surface zone that show improved chemical stability, electrical conductivity, biochemical and catalytic activities when compared with larger-than-nanoscale structures of similar composition<sup>1-2</sup>. Silver nanoparticles have therefore found potential applications as functional units of electronic sensors and optical devices, antimicrobial agents, biological sensors and industrial catalysts<sup>1,3,4</sup>. The catalytic activity of AgNPs have been employed in the degradation of organic dyes used in industries such as the pharmaceutical, food, textile, paper and print<sup>5-6</sup>. Organic dyes when discharged into wastewater without proper or adequate treatment persist in the ecosystem and can constitute, in addition to severe ecological disruption, health hazards to human. Majority of conventional wastewater treatment methods that have been employed such as flocculation, coagulation, electrochemical degradation, precipitation, adsorption and reverse osmosis remain expensive and often lead to secondary pollution because of excessive use of reagents required to destroy the aromatic stability of the dye<sup>6</sup>. Nanocatalysts, which lower the activation energy required for the breakdown of the organic dyes, will be useful in the safe, efficient and affordable disposal of these environmental chemical hazards. In this regard, several studies have demonstrated the potential application of AgNPs in the degradation of synthetic dyes including methylene blue and methyl orange<sup>5,7,8</sup>. Silver nanoparticles are unique in nanoscale system due to the ease in its synthesis and chemical modifications. Chemical reduction of silver ions remains the most viable means of synthesizing AgNPs with the use of a variety of organic and inorganic reducing agents reported in literature<sup>9</sup>. However, the green synthesis of AgNPs using microorganisms and plants is preferred because the approach is eco-friendly, energy saving and easily scalable. In addition, the presence of plants metabolites as capping agents allow the synthesis of nanoparticles with predefined characteristics<sup>4</sup>. Silver nanoparticles have therefore been successfully biosynthesized using microorganisms including *Ganoderma enigmaticum*<sup>10</sup>, *Oscillatoria limnetica*<sup>11</sup> as well as parts from plants such as *Phyllanthus emblica*<sup>12</sup>, *Cucumis prophetarum*<sup>4</sup>, *Salvia spinosa*<sup>13</sup>.

*Euphorbia graminea* Jacq (Euphorbiaceae) is an annual plant in Nigeria measuring 15-30 cm from the base with leaves that are alternate and may be ovate or oblong, elliptic to linear <sup>14</sup>. The plant which has been previously described as a potentially invasive herbaceous plant in Nigeria has been documented to possess antioxidant activity as well as antiproliferative potential against human breast (MCF-7) cancer cell lines <sup>15,16</sup>. Antimicrobial screening of chromatographic fractions of the plant showed mild inhibitory activity against *Staphylococcus aureus*, *E. coli* and *Candida albicans* <sup>14</sup>. The phytochemicals obtained from the plant include alkaloids, anthraquinones, flavonoids, tannins and terpenes. Biomolecules containing hydroxyl and carbonyl functional groups can serve as reducing and stabilizing agents in the synthesis of AgNPs from ions.

The objective of this study was therefore to employ the aqueous extract of the whole plant of *Euphorbia graminea* in the green synthesis of AgNPs that possess antimicrobial and catalytic activities.

## METHODOLOGY

### Materials

*Euphorbia graminea* was collected from the botanical garden of the University of Ibadan, Ibadan. A trained botanist authenticated the collected plant sample, and a voucher specimen (UIH-23130) was deposited for future reference. Silver nitrate was sourced from Sigma Aldrich while methylene blue and sodium borohydride were products of BDH UK.

### Preparation of *E. graminea* extract

The stem and leaves of *E. graminea* were thoroughly washed with distilled water and then cut into small pieces with the aid of a steel knife. A quantity of the plant parts equal to 40 g was heated with 400 mL of distilled water in a beaker at 60 for 30 minutes <sup>2</sup>. On cooling, the mixture was filtered using Whatman filter paper No.1 and the filtrate stored in amber-colored bottles at 4 until required.

### Phytochemical screening of extract *E. graminea*

Preliminary phytochemical screening was carried out on freshly prepared plant extract to determine presence of phenols, tannins, flavonoids, triterpenoids, and alkaloids using standard procedures <sup>2,4</sup>.

### Synthesis of Ag-NP using aqueous *E. graminea*

The optimized procedure involved the addition of 10 mL of the aqueous extract to 90 mL of 1 mM AgNO<sub>3</sub> in a conical flask covered with aluminum foil.

The reaction mixture was then continuously stirred at about 1000 rpm using a magnetic stirrer for 24 hours. The reduction of silver ions to AgNPs was monitored by acquiring UV-visible data of aliquots taken from the reaction mixtures at regular intervals. Preliminary visual check of color change from light green to brownish-red in the reaction mixture was also used to monitor reduction <sup>1</sup>.

After completion of the reaction, nanoparticles were purified by first centrifuging the mixture at 15,000 rpm for 5 minutes to obtain pellets. The pellet was re-dispersed in distilled water using a vortex mixer and then centrifuged. Washing with water was done thrice and then with ethanol.

### **Optimization of AgNO<sub>3</sub> concentration**

While keeping the ratio of volumes of the extract to silver nitrate solution as 1:9, the effect of the concentration of silver nitrate solution on formation of nanoparticles was investigated by varying its concentration (0.25, 0.5 and 1mM).

### **Optimization of ratio of volumes of AgNO<sub>3</sub> and extract**

Extract-to-silver nitrate volume ratios of 1:9; 3:7 and 5:5 were differently employed for nanosynthesis in order to determine the ratio of volumes optimal for nanoparticle formation.

### **Characterization of synthesized AgNPs**

UV-visible spectroscopic data of the reaction mixture were acquired at regular intervals using a Perkin Elmer Lambda 250 Model in the range of 200-800 nm and 1 nm resolution. The functional groups present in the phytoconstituents of the plant that were responsible for the reduction and capping of nanoparticles were analyzed by FT-IR measurements using a Nicolet iS10 FT-IR spectrophotometer. The size and morphology of the AgNPs were determined by Transmission Electron Microscope (NanoMill 1040 model) while the elemental composition was analyzed using scanning electron microscope integrated with energy dispersive X-ray analysis. Dynamic light scattering (DLS) data were acquired at 25°C using Malvern Zetasizer NanoS90 (UK) with a detector set at right angles <sup>2</sup>.

The crystallinity of the biosynthesized AgNPs was confirmed by XRD analysis using Cu K alpha radiation set at 40kV and 20mA.

### **Antimicrobial Assay of phytosynthesized AgNPs**

The antimicrobial screening of the phytosynthesized AgNPs was carried out by determining the minimum inhibitory and bactericidal/fungicidal concentrations against seven test microorganisms including: one Gram-positive (*Staphylococcus aureus* – ATCC 29213), five Gram-negative bacteria (*Klebsiella*

*pneumoniae* – ATCC 7006303, *Clostridium faecalis* – ATCC 8090, *Escherichia coli* - 2348, *Salmonella typhi* – ATCC 14028 and *Pseudomonas aeruginosa* – ATCC 27853) and one fungi (*Candida albicans*). The minimum inhibitory concentration of the as-synthesized AgNPs against the test microorganisms was carried out as described by Mogana et al., 2020<sup>17</sup> with some modifications using broth micro-dilution method in 96-well microtiter plates. Bacteria and fungi stock suspensions were diluted using Mueller Hinton broth and tryptic Soy broth respectively to give 0.5 McFarland standard. To each of the well containing graded concentrations of AgNPs corresponding to 500, 250, 125, 62.5, 31.25, 15.63, 7.81, 3.91, 1.95 and 0.98 µg/mL, 20 of the standardized microbial suspension were added and incubated at 37°C for 24 hours for bacteria and at 25°C for up to 48 – 72 hours for fungi. A check for microbial growth in each well was done. The minimum bactericidal/fungicidal concentration (MBC/MFC) for the test samples was determined by swabbing broth from the 96-well plates that did not show any visible growth on the surface of freshly prepared Mueller Hinton (for bacteria) and Sabouraud dextrose (for fungi) agar plates by surface spreading method using sterile cotton swabs. The plates were thereafter incubated at 37°C for up to 72 hours. The lowest concentration of the test sample from the MIC assay that that did not show any microbial growth on the agar plates were taken as the MBC/MFC for that organism<sup>10</sup>.

### **Catalytic activity of as-synthesized AgNPs**

The biocatalytic efficiency of synthesized AgNPs in the borohydride-reduction of methylene blue was investigated by monitoring the degradation of the dye with time <sup>3,6</sup>. Reaction variables including the concentrations of sodium borohydride, methylene blue and AgNPs were optimized. In the final optimized procedure, 5mL of 10mM methylene blue was added to 2mL of 0.2M sodium borohydride and the volume made up to 50 mL with distilled water after which 10 mg AgNPs was added. The absorption spectra of aliquots periodically drawn from the reaction mixture was then acquired. A blank set up without the nanocatalyst was similarly prepared and analyzed.

## **RESULTS AND DISCUSSION**

### **Phytochemical Analysis**

The phytochemical analysis of the plant extract revealed the presence of several phytoconstituents as shown in Table 1. Similar phytochemical composition of the plant has been previously reported <sup>14</sup>. These secondary metabolites mediate the reduction of silver ions and capping of resultant AgNPs.

**Table 1.** Phytochemical constituents of aqueous extract of *E. graminea*

Secondary metabolite	Quantitative presence
Tannins	+
Flavonoids	+
Cardiac glycosides	++
Saponins	++
Terpenoids	++
Phenol	+
Alkaloids	++

### Synthesis and optimization of reaction variables

The bioreduction of silver ions to AgNPs was associated with a color change from greenish yellow of the plant extract to deep red as the AgNPs were formed. The color of colloidal solutions of AgNPs have been reported to vary depending on their particle size and morphology<sup>18</sup>. This in turn often depends on the conditions of synthesis. UV spectroscopy was therefore utilized to monitor biosynthesis as AgNPs can interact with light of specific wavelengths thereby causing the conduction electrons on the surface of the metal to collectively oscillate in a phenomenon known as surface plasmon resonance. As depicted in Figure 1, the surface plasmon resonance of AgNPs biosynthesized using aqueous extract of *E. graminea* occurred at 462 nm, suggestive of a particle size of about 70 nm<sup>18</sup>. However, the actual particle size will be determined using TEM and XRD analyses. The use of 1mM silver nitrate solution was critical to formation of small-sized AgNPs in high yields as the use of lower concentrations resulted either in lower yields or bathochromic shifts of the surface plasmon resonance that is indicative of the formation of larger-sized nanoparticles.

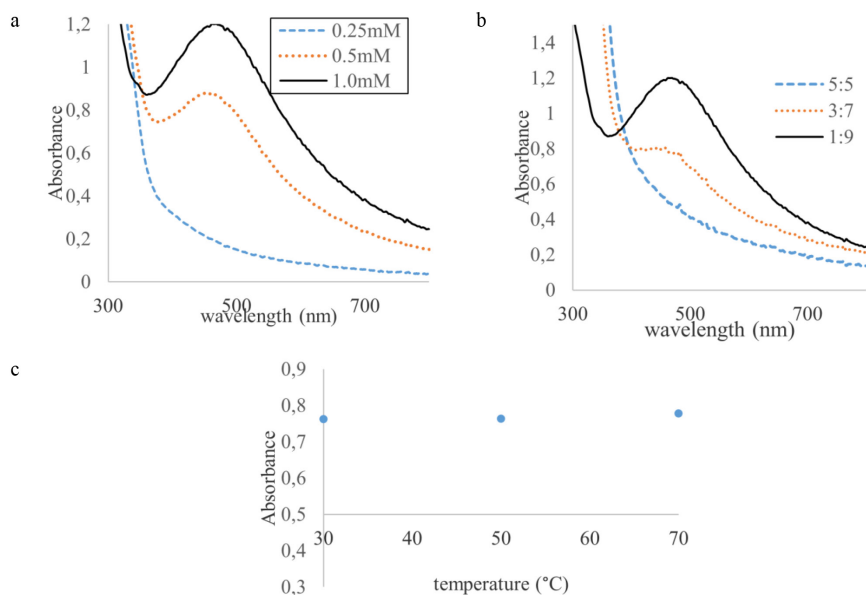


**Figure 1.** Optimization of critical reaction parameters including (a) concentration of  $\text{AgNO}_3$  (b) extract-to- $\text{AgNO}_3$  volume ratios and (c) temperature

Similarly, an extract-to-silver nitrate volume ratio of 1:9 was found optimal in the biosynthesis of smaller-sized AgNPs in high yields as shown in Figure 1b. As depicted in Figure 1c, no advantage, as regard the particle size or yields, were observed when the reaction was conducted at higher temperatures and as such 30 was adopted for the synthesis.

## Characterization of biosynthesized AgNPs

### FT-IR Measurement

FTIR analysis was carried out to identify the likely phytochemicals involved in the bioreduction of silver ions to Ag and capping of the AgNPs biosynthesized from the aqueous extract of *E. graminea*. The FTIR spectra of the AgNPs is depicted in Figure 2 below.

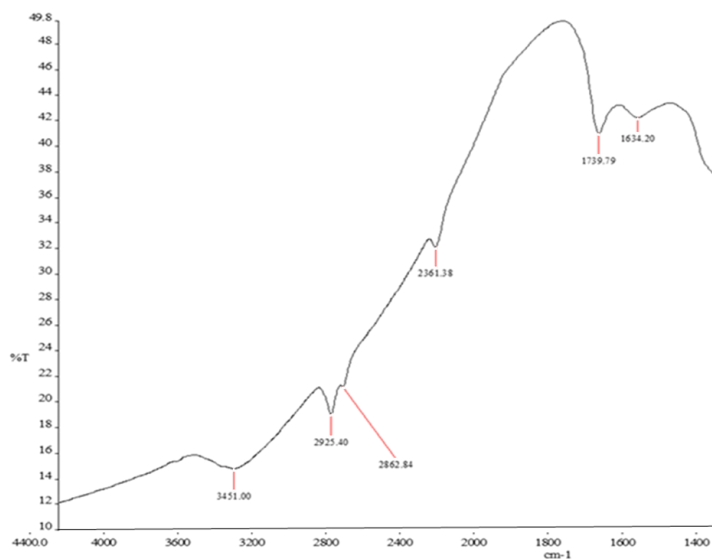


**Figure 2.** FTIR spectrum of biosynthesized AgNPs using *E. graminea* aqueous extract

Broad and strong peaks at  $3451\text{cm}^{-1}$  can be attributed to the O-H stretch of phenolic compounds. This could also be attributed to hydrogen-bonded O-H stretch of alcohols or N-H stretch of amine salts. The bands at  $2925.40$  and  $1634.20\text{ cm}^{-1}$  have been assigned to C-H stretching and bending vibrations respectively of conjugated alkenes. The latter frequency could also designate N-H bending vibrations of amines or their salts which characteristically are found between  $1650$  and  $1580\text{ cm}^{-1}$  depending on their chemical environment<sup>5</sup>. The medium bands at  $2862.84\text{ cm}^{-1}$  corresponds to C-H stretch frequencies in  $\text{sp}^3$  hybridized hydrocarbons. Thus, the biosynthesized AgNPs are surrounded by metabolites such as terpenoids and flavonoids with functional groups of alcohols, alkanes, alkenes, and amines. These functional residues showed the capability to stabilize and prevent further agglomeration of biosynthesized AgNPs<sup>19</sup>.

### SEM and EDX analyses

When the green-synthesized nanoparticles were examined using SEM, they appeared as highly aggregated polymorphs with shapes mostly irregularly granulated as shown in Figure 3a. Similar results were obtained with the biosynthesis of AgNPs using *Cucumis prophetarum*<sup>4</sup>.

The characterization of the biosynthesized AgNPs by EDX analysis revealed the presence of the characteristic peak of elemental silver as depicted in Figure 3b. The as-synthesized AgNPs displayed an absorption band at  $3\text{KeV}$  which is typical of metallic silver nanoparticles as a result of their surface plasmon resonance<sup>20</sup>.

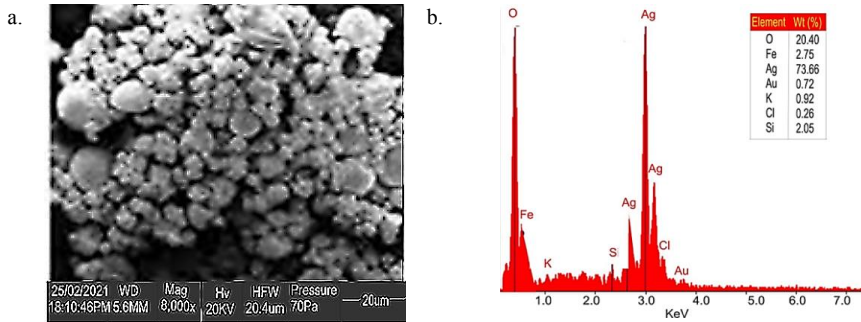


**Figure 3.** SEM (a) and EDX (b) Analyses of AgNPs biosynthesized using *E. graminea*

The elemental analysis of the biosynthesized AgNPs revealed the predominance (73.66%) of elemental silver particles confirming the high efficiency of *E. graminea* as a reductant of silver ions. In addition to silver, other elements including oxygen, iron, silicon etc. were also present.

### Determination of AgNPs size and morphology by TEM

The TEM micrograph as depicted in Figure 4 revealed well-separated, quasi-spherical shaped AgNPs. The average particle size of the AgNPs as determined by TEM was  $6.77 \pm 0.89$  nm. When compared with previously reported AgNPs size ranges of 12-36, 11-83 and 10-180 nm that were obtained using *Ficus panda*, *Terminalia mentaly* and *Clinacanthus nutans* respectively, our new method successfully produced small sized nanoparticles with narrower size distribution <sup>2,19,20</sup>.

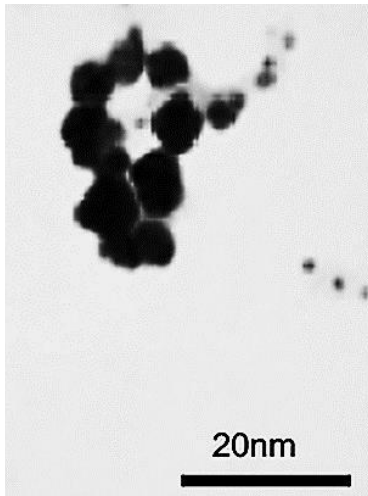


**Figure 4.** Transmission electron microscopy of biosynthesized AgNPs

## Dynamic light scattering analysis

Dynamic light scattering (DLS) measures the correlation coefficient of intensity functions which can be mathematically converted to intensity, volume, or number size distribution<sup>21-22</sup>. The technique is very useful for estimating particle size via the analysis of the modulation of the intensity of laser light passing through a colloidal solution. The particle size distribution of the biosynthesized nanoparticles was therefore determined using DLS with the size distribution by intensity depicted in Figure 5. The DLS data showed that the Z-average size of the particles was 43.14 nm with a polydispersity index of 0.467. The polydispersity index (values 0 to 1) describes the width of particle size distribution with scale ranging from monodisperse to polydisperse particles. Monodispersity arises from zeta potential values that are more negative than -30 mV or more positive than 30 mV and is thus indicative of nanoparticles colloid stability<sup>4,21</sup>. The particle size estimated by DLS was expectedly larger than the nominal size by TEM<sup>23</sup>. This is because DLS measure the hydrodynamic size which is dependent on particle morphology. In particular, intensity-sized distribution can be strongly influenced by the presence of a few large particles, aggregates or dust<sup>24</sup>. In addition, the hydration layer around the nanoparticles and the phytochemicals of the extract may contribute to the hydrodynamic size<sup>4</sup>.

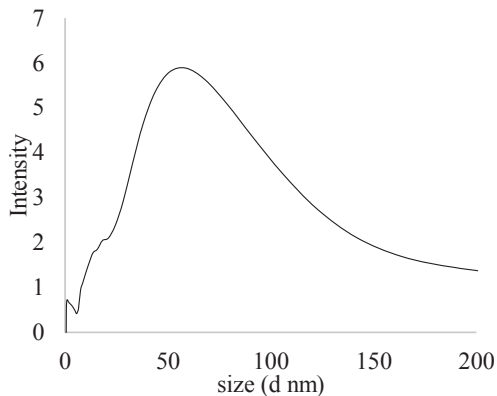


**Figure 5.** Size distribution of biosynthesized AgNPs by intensity

## Crystallinity of AgNPs using XRD

As depicted in Figure 6, the XRD pattern of the biosynthesized AgNPs revealed four intense peaks at  $2\theta = 38.21, 44.43, 64.79$  and  $77.86$  which corresponds to (111), (200), (220) and (311) lattice planes. The observed lattice planes were indexed based on the face centered cubic structure of silver as found in standard

data file JCPDS No. 04-0783. The XRD pattern thus clearly confirmed the crystallinity of the AgNPs synthesized in this study. The maximum intensity was observed with the (111) plane indicating the AgNPs were predominantly distributed in the (111) plane.

The average crystallite size of the AgNPs was calculated using the Debye-Scherrer formula below

$$d = \frac{0.9\lambda}{\beta \cos\theta} \quad (1)$$

where,  $d$  is the mean crystallite diameter,  $\lambda$  is the X-ray wavelength,

The mean crystallite size of the silver nanoparticles was determined to be 7.65 nm.

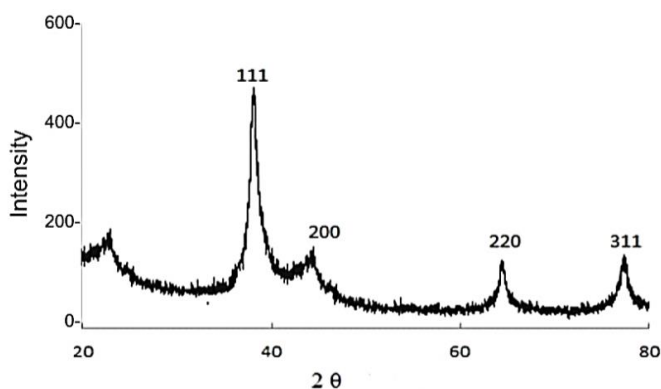


**Figure 6.** XRD pattern of biosynthesized AgNPs

### **Antimicrobial assay**

The antimicrobial activities of the green-synthesized AgNPs against the various test organisms are shown in Table 2. The AgNPs exhibited broad-spectrum activity against both Gram positive and negative bacteria as well as fungi.

**Table 2.** Minimum Inhibitory and bactericidal/fungicidal concentrations of green-synthesized AgNPs against test organisms

Test organisms	Minimum Inhibitory Concentration (µg/mL)	Minimum Bactericidal/Fungicidal Concentration (µg/mL)
<i>Klebsiella pneumonia</i> – ATCC 7006303	125	250
<i>Pseudomonas aeruginosa</i> – ATCC 27853	31.25	500
<i>Staphylococcus aureus</i> – ATCC 29213	125	125
<i>Escherichia coli</i> - 2348	31.25	125
<i>Salmonella typhi</i> – ATCC 14028	62.5	125
<i>Clostridium faecalis</i> – ATCC 8090	31.25	250
<i>Candida albicans</i>	62.5	>500

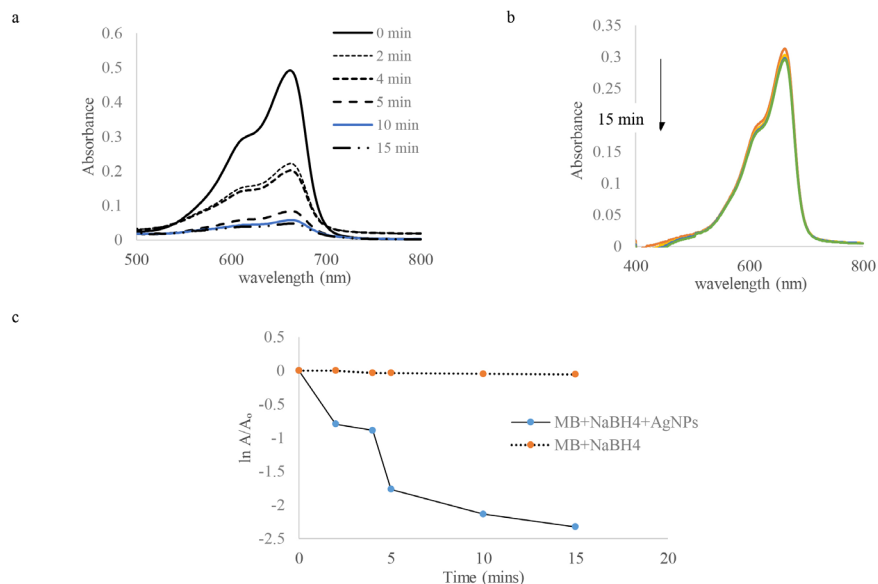
The antimicrobial activity of the biogenic AgNPs were more pronounced against Gram-negative bacteria including *P. aeruginosa*, *E. coli* and *C. faecalis* (MIC 31.25 /mL) than Gram-positive *S. aureus* with MIC of 125 µg/mL. This pattern can be attributed to the mechanism of antibacterial activity of AgNPs that involves the electrostatic attraction and transfer of silver ions to the negatively charged bacteria cell wall leading to a change in its composition and permeability<sup>25</sup>. The combined effect of the subsequent loss in the ability of the organism's DNA to replicate and the inactivation of enzymes required for ATP production will eventually lead to bacterial death. Gram-negative bacteria with a single layer of peptidoglycan in their cell wall membrane are therefore more susceptible to the inactivating action of silver ions than Gram-positive bacteria with multiple layered peptidoglycan cell membrane<sup>4</sup>. Many previous works have only reported inhibitory activity of biosynthesized AgNPs against only two to four microorganisms. In contrast, the as-synthesized AgNPs reported in this study exhibited a broader range of activity against microorganisms including fungi. A survey of the MIC values reported for AgNPs synthesized using different plant extracts against the more commonly tested *S. aureus* and *P. aeruginosa* is depicted in Table 3. The results showed the considerable inhibitory effect of AgNPs synthesized using *E. graminea* and the potential of the nanoparticles for future antibacterial applications.

**Table 3.** A comparison of the antibacterial activity of different plant-mediated AgNPs

Plant used	Mean particle size	MIC		Reference
		<i>S. aureus</i>	<i>P. aeruginosa</i>	
<i>Camellia sinensis</i>	3.9±1.6	250	30	26
<i>Crocus sativus</i>	12-20	No inhibition	250	27
<i>Crocus Haussknechtii Bois</i>	10-25	26.9	20.2	28
<i>Terminalia mentaly</i>	11-83	12.5	Not reported	20
<i>Euphorbia graminea</i>	6.77±0.89	125	31.25	This study

### AgNP-catalysed degradation of methylene blue

The biocatalytic activity of as-synthesized AgNPs in the redox reaction between methylene blue and borohydride ions was also investigated. The progressive degradation of methylene blue characterized by loss of its intense blue color was monitored by acquisition of the UV-visible spectra data of the reaction mixture at regular time intervals. The changes in the UV-visible spectra of methylene blue in the presence and absence of the nanocatalyst are depicted in Figure 7a and 7b respectively. Both reactions fitted a pseudo first order kinetics model as shown in Figure 7c.

**Figure 7.** Successive acquisition of UV-visible spectra at specified time intervals showing reduction of methylene blue by NABH<sub>4</sub> at ambient temperature: (a) with nanocatalyst, (b) without nanocatalyst and (c) plots of against time

Rate constants were estimated from the regression of relative absorbances of the dye with time. The rate constant of the degradation of methylene blue in the presence of nanocatalyst was  $\text{sec}^{-1}$  compared to  $\text{sec}^{-1}$  in the absence of the nanocatalyst. The rate of degradation of the dye was therefore several folds faster in the presence of nanocatalyst with more than 90% degradation achieved within 15 minutes. In contrast, less than 6% degradation was achieved in that time without the inclusion of AgNPs as catalyst.

Degradation of methylene blue requires an electron transfer from borohydride ions to the dye. The nanocatalyst serve as an intermediate in the electron transfer process between the acceptor and donor molecules <sup>19</sup>. The mechanism of catalysis by AgNPs therefore involve an improvement in the efficiency of electron transfer as well as the lowering of the bond dissociation energy during the chemical reaction between the dye and borohydride ions that is required for breaking/forming of bonds. As depicted in Table 4, when compared with other studies, AgNPs biosynthesized using *E. graminea* exhibited excellent catalytic efficiency. The enhanced catalytic efficiency can be attributed to the nanoparticles' quasi-spherical shape and small size that have been reported to improve catalytic efficiency. Similarly, the presence of hetero atoms such as oxygen, which is the next most abundant element (20.40% in EDX analysis) in the phytochemical-capped nanoparticles, have been reported to improve the access of the dye molecules to the catalytic sites leading to accelerated degradation <sup>6</sup>.

**Table 4.** A comparison of catalytic efficiency of biosynthesized AgNPs

Plant used	Mean particle size (nm)	Rate constant	Time of degradation (at least 90%)	Reference
<i>Alstonia scholaris</i>		50 0.0007 $\text{sec}^{-1}$ Not specified		29
<i>Caulerpa racemosa</i>	25	0.0011 $\text{sec}^{-1}$	30 min	30
<i>Imperata cylindrica</i>	31	0.137 $\text{min}^{-1}$	14 min	31
<i>Euphorbia graminea</i>	6.8	0.0025 $\text{sec}^{-1}$	15 min	This study

In conclusion, a facile, eco-friendly process involving the use of aqueous extract of *E. graminea* for the green synthesis of stable silver nanoparticles has been developed. The nanoparticles were crystalline, predominantly quasi-spherical shaped and with an average particle size of  $6.77 \pm 0.89$  nm. The prepared AgNPs showed good catalytic activity in the sodium borohydride-degradation of meth-

ylene blue as well broad-spectrum antimicrobial activity against bacteria and fungi. The nanoparticles can therefore find useful applications in the effluent treatment of chemical industries and as therapeutic coats in medical devices.

#### **STATEMENT OF ETHICS**

Not applicable as no human or animal subjects were involved in the study.

#### **CONFLICT OF INTEREST**

The authors declare there is no conflict of interest associated with this study.

#### **AUTHOR CONTRIBUTIONS**

OET was involved in study design, data collection, analysis, and preparation of manuscript draft. OSA and PEO were involved in data collection and analysis. All authors contributed to the revision of the draft, read, and approved the final manuscript.

#### **FUNDING SOURCES**

No funding or other financial support was received for this study.

## REFERENCES

1. Rafique M, Sadaf I, Rafique MS, Tahir MB. A review on green synthesis of silver nanoparticles and their applications. *Artif. Cells Nanomed. Biotechnol.*, 2017; 45(7): 1272–1291. <https://doi.org/10.1155/2015/682749>
2. Yusuf SN, Mood CN, Ahmad NH, Sandai D, Lee CK, Lim V. Optimization of biogenic synthesis of silver nanoparticles from flavonoid- rich *Clinacanthus nutans* leaf and stem aqueous extracts. *R. Soc. Open Sci.*, 2020; (7): 200065. <https://doi.org/10.1098/rsos.200065>
3. Saha J, Begum A, Mukherjee A, Kumar S. A novel green synthesis of silver nanoparticles and their catalytic action in reduction of Methylene Blue dye. *Sustain Environ. Res.*, 2017; 27(5): 245–250. <https://doi.org/10.1016/j.serj.2017.04.003>
4. Hemlata, Meena PR, Singh AP, Tejavath KK. Biosynthesis of silver nanoparticles using *cucumis prophetarum* aqueous leaf extract and their antibacterial and antiproliferative activity against cancer cell lines. *ACS Omega*, 2020; 5(10): 5520–5528. <https://doi.org/10.1021/acsomega.0c00155>
5. Al-Zaban MI, Mahmoud MA, AlHarbi MA. Catalytic degradation of methylene blue using silver nanoparticles synthesized by honey. *Saudi J. Biol. Sci.*, 2021; 28(3):2007–2013. <https://doi.org/10.1016/j.sjbs.2021.01.003>
6. Sharma K, Singh G, Kumar M, Bhalla V. Silver nanoparticles: Facile synthesis and their catalytic application for the degradation of dyes. *RSC Adv.*, 2015; 5(33): 25781–25788. <https://doi.org/10.1039/c5ra02909k>
7. Atta AM, Moustafa YM, Al-Lohedan HA, Ezzat AO, Hashem AI. Methylene blue catalytic degradation using silver and magnetite nanoparticles functionalized with a poly (ionic liquid) based on quaternized dialkylethanolamine with 2-acrylamido-2-methylpropane sulfonate-co-vinylpyrrolidone. *ACS Omega*, 2020; 5(6): 2829–2842. <https://doi.org/10.1021/acsomega.9b03610>
8. Cyril N, George JB, Joseph L, Sylas VP. Catalytic degradation of methyl orange and selective sensing of mercury ion in aqueous solutions using green synthesized silver nanoparticles from the seeds of *Derris trifoliata*. *J Clust Sci* 2019; 30(2): 459–468. <https://doi.org/10.1007/s10876-019-01508-9>
9. Ahmad S, Munir S, Zeb N, Ullah A, Khan B, Ali J, et al. Green nanotechnology: a review on green synthesis of silver nanoparticles—an ecofriendly approach. *Int. J. Nanomedicine* 2019; 14: 5087. <https://doi.org/10.2147/IJN.S200254>
10. Gudikandula K, Vadapally P, Charya MAS. Biogenic synthesis of silver nanoparticles from white rot fungi: their characterization and antibacterial studies. *OpenNano*, 2017; 2: 64–78. <https://doi.org/10.1016/j.onano.2017.07.002>
11. Hamouda RA, Hussein MH, Abo-Elmagd RA, Bawazir SS. Synthesis and biological characterization of silver nanoparticles derived from the cyanobacterium *Oscillatoria limnetica*. *Sci. Rep.*, 2019; 9(1): 1–17. <https://doi.org/10.1038/s41598-019-49444-y>
12. Masum MMI, Siddiq MM, Ali KA, Zhang Y, Abdallah Y, Ibrahim E, et al. Biogenic synthesis of silver nanoparticles using *Phyllanthus emblica* fruit extract and its inhibitory action against the pathogen *Acidovorax oryzae* strain RS-2 of rice bacterial brown stripe. *Front Microbiol.*, 2019; 10: 820. <https://doi.org/10.3389/fmicb.2019.00820>
13. Pirtarighat S, Ghannadnia M, Baghshahi S. Green synthesis of silver nanoparticles using the plant extract of *Salvia spinosa* grown in vitro and their antibacterial activity assessment. *J. Nanostructure Chem.*, 2019; 9(1): 1–9. <https://doi.org/10.1007/s40097-018-0291-4>

14. Ikpefan EO, Enwa FO, Emebrado O. *Euphorbia graminea* Jacq. (Euphorbiaceae): The antimicrobial assessment of the extract and fractions of the leaves. *Niger J. Pure Appl. Sci.*, 2020; 33(2): 3809–3818. <http://dx.doi.org/10.48198/NJPAS/20.B15>
15. Aigbokhan EI, Eku O. Aspects of the biology and ecology of *Euphorbia graminea* Jacq. (Euphorbiaceae) – a potentially invasive herbaceous plant in Nigeria. *Niger J. Bot.*, 2015; 1: 35–53.
16. Ikpefan EO, Ayinde BA, Mudassar A, Farooq AD. *In vitro* antiproliferative and antioxidant assessment of the extract and partitioned fractions of leaves of *Euphorbia graminea* Jacq. (Euphorbiaceae). *Niger J. Pharm.*, 2020; 53(3): 55–62. <https://doi.org/10.51412/psn-njp.2021.5>.
17. Mogana R, Adhikari A, Tzar MN, Ramliza R, Wiart C. Antibacterial activities of the extracts, fractions and isolated compounds from *Canarium patentinervium* Miq. against bacterial clinical isolates. *BMC Complement Med. Ther.*, 2020; 20(1): 1–11. <https://doi.org/10.1186/s12906-020-2837-5>
18. Paramelle D, Sadovoy A, Gorelik S, Free P, Hobley J, Fernig DG. A rapid method to estimate the concentration of citrate capped silver nanoparticles from UV-visible light spectra. *Analyst* 2014; 139(19): 4855–4861. <https://doi.org/10.1039/C4AN00978A>
19. Tripathi RM, Kumar N, Shrivastav A, Singh P, Shrivastav BR. Catalytic activity of biogenic silver nanoparticles synthesized by *Ficus panda* leaf extract. *J. Mol. Catal.* 2013; 96: 75–80. <https://doi.org/10.1016/j.molcatb.2013.06.018>
20. Majoumouo MS, Sibuyi NRS, Tincho MB, Mbekou M, Boyom FF, Meyer M. Enhanced anti-bacterial activity of biogenic silver nanoparticles synthesized from *Terminalia mantaly* extracts. *Int. J. Nanomedicine* 2019; 14: 9031–46. <https://doi.org/10.2147/IJN.S223447>
21. Wong JC, Xiang L, Ngoi KH, Chia CH, Jin KS, Ree M. Quantitative structural analysis of polystyrene nanoparticles using synchrotron X-ray scattering and dynamic light scattering. *Polymers* 2020; 12: 1–16. <https://doi.org/10.3390/polym12020477>
22. Elamawi RM, Al-Harbi RE, Hendi AA. Biosynthesis and characterization of silver nanoparticles using *Trichoderma longibrachiatum* and their effect on phytopathogenic fungi. *Egypt. J. Biol. Pest Control* 2018; 28(1): 1–11. <https://doi.org/10.1186/s41938-018-0028-1>
23. Jang MH, Lee S, Hwang YS. Characterization of silver nanoparticles under environmentally relevant conditions using asymmetrical flow field-flow fractionation (AF4). *PLoS One* 2015; 10(11): e0143149. <https://doi.org/10.1371/journal.pone.0143149>
34. Vega-Baudrit J, Gamboa SM, Rojas ER, Martinez VV. Synthesis and characterization of silver nanoparticles and their application as an antibacterial agent. *Int. J. Biosens. Bioelectron.*, 2019; 5(5): 166–73. <https://doi.org/10.15406/ijbsbe.2019.05.00172>
25. Agnihotri S, Mukherji S, Mukherji S. Immobilized silver nanoparticles enhance contact killing and show highest efficacy: elucidation of the mechanism of bactericidal action of silver. *Nanoscale* 2013; 5(16): 7328–40. <https://doi.org/10.1039/C3NR00024A>
26. Rolim WR, Pelegrino MT, de Araújo Lima B, Ferraz LS, Costa FN, Bernardes JS, Rodrigues T, Brocchi M, Seabra AB. Green tea extract mediated biogenic synthesis of silver nanoparticles: characterization, cytotoxicity evaluation and antibacterial activity. *Appl. Surf. Sci.*, 2019; 463: 66–74. <https://doi.org/10.1016/j.apsusc.2018.08.203>
27. Bagherzade G, Tavakoli MM, Namaei MH. Green synthesis of silver nanoparticles using aqueous extract of saffron (*Crocus sativus* L.) wastages and its antibacterial activity against six bacteria. *Asian Pac. J. Trop. Biomed.*, 2017; 7: 227–233. <https://doi.org/10.1016/j.apjtb.2016.12.014>

28. Mosaviniya M, Kikhavani T, Tanzifi M, Yaraki MT, Tajbakhsh P, Lajevardi A. Facile green synthesis of silver nanoparticles using *Crocus Haussknechtii* Bois bulb extract: Catalytic activity and antibacterial properties. *Colloids Interface Sci. Commun.*, 2019; 33: 100211. <https://doi.org/10.1016/j.colcom.2019.100211>
29. Rajasekar R, Samuel M, Edison TNJI, Raman N. Sustainable synthesis of silver nanoparticles using *Alstonia scholaris* for enhanced catalytic degradation of methylene blue. *J. Mol. Struct.*, 2021; 1246: 131208. <https://doi.org/10.1016/j.molstruc.2021.131208>
30. Edison TNJI, Atchudan R, Kamal C, Lee YR. *Caulerpa racemosa*: a marine green alga for eco-friendly synthesis of silver nanoparticles and its catalytic degradation of methylene blue. *Bioprocess Biosyst. Eng.*, 2016; 39(9): 1401–1408. <https://doi.org/10.1007/s00449-016-1616-7>
31. Fairuzi AA, Bonnia NN, Akhir RM, Abrani MA, Akil HM. Degradation of methylene blue using silver nanoparticles synthesized from *imperata cylindrica* aqueous extract. In *IOP Conf. Ser.: Earth Environ. Sci.* IOP Publishing 2018; 105(1): 012018. <https://doi.org/10.1088/1755-1315/105/1/012018>